CRYSTAL GROWTH & DESIGN

pubs.acs.org/crystal Article

Incorporating Ester Functionality within a Solid-State [2 + 2] Cycloaddition Reaction Based Upon Halogen Bonding Interactions

Published as part of a Crystal Growth and Design virtual special issue on Crystalline Molecular Materials: From Structure to Function

Samantha J. Kruse, Eric Bosch,* Fayeshun Brown, and Ryan H. Groeneman*

Cite This: *Cryst. Growth Des.* 2020, 20, 1969–1974 Read Online

ACCESS | Metrics & More | Article Recommendations | Supporting Information

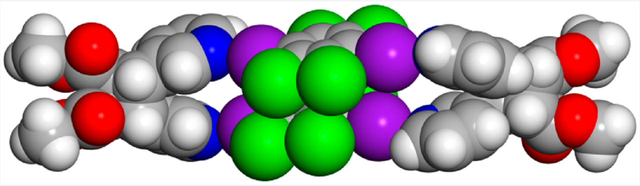

ABSTRACT: The formation of cocrystals based upon 1,4-diiodoperchlorobenzene ($C_6I_2Cl_4$) as a halogen bond donor along with a series of isomeric pyridine vinyl esters, namely, (*E*)-methyl-3-(pyridine-*X*-yl)prop-2-enoate (where X = 4, 3, and 2) (4-PAMe), (3-PAMe), and (2-PAMe), has been achieved. In all cases, $C_6I_2Cl_4$ halogen bonds to a combination of pyridine nitrogen atoms as well as ester oxygen atoms to yield an extended solid. The cocrystals $(C_6I_2Cl_4)\cdot$(4-PAMe) and $(C_6I_2Cl_4)\cdot 2$(3-PAMe) were observed to be photoreactive. X-ray structural analysis revealed that molecules of $C_6I_2Cl_4$ are stacked in a homogeneous face-to-face $\pi-\pi$ orientation which then positions a pair of carbon–carbon double bonds (C=C) in the correct orientation to undergo a solid-state [2 + 2] cycloaddition reaction. Thus, upon exposure to ultraviolet light, both $(C_6I_2Cl_4)\cdot$(4-PAMe) and $(C_6I_2Cl_4)\cdot 2$(3-PAMe) undergo a regioselective and quantitative photoreaction to yield the head-to-head photoproduct, namely, (*rctt*)-dimethyl-3,4-bis(pyridine-4-yl)cyclobutane-1,2-dicarboxylate and (*rctt*)-dimethyl-3,4-bis(pyridine-3-yl)cyclobutane-1,2-dicarboxylate, respectively. X-ray analysis of $(C_6I_2Cl_4)\cdot$(2-PAMe) revealed the structural reason behind the observed photostability which is attributed to the large parallel displacement of the double bonds.

INTRODUCTION

Halogen bonding continues to be a reliable and highly investigated noncovalent interaction in the formation of numerous multicomponent molecular solids.[1−3] Akin to hydrogen bonding, halogen bonding has been utilized in the formation of cocrystals in order to control various properties of these solids.[4] An area within halogen bonding cocrystals that is not well researched, when compared to hydrogen bonding, is in the area of solid-state photochemistry in terms of the [2 + 2] cycloaddition reaction. Surprisingly, the number of photoreactive cocrystals based upon halogen bonding interactions is still very limited.[5−7] A continued focus of our research groups is to achieve a solid-state [2 + 2] cycloaddition reaction within multicomponent solids based upon halogen bonding interactions. Previously, we have reported a series of photoreactive cocrystals based upon 1,4-diiodoperchlorobenzene ($C_6I_2Cl_4$) as a halogen bond donor along with *trans*-1,2-bis(4-pyridyl)ethylene (4,4′-BPE)[8] and 4-stilbazole (4-SB)[9] as reactant molecules. In each cocrystal, an extended solid was observed based upon I···N halogen bonds that positioned a pair of carbon–carbon double bonds (C=C) in the correct orientation to undergo a photoreaction in the solid state.

Aligned with the goals of our research, we report here the incorporation of an organic functionality, namely, the ester group, within a pair of photoreactive cocrystals based upon halogen bonding interactions. In particular, $C_6I_2Cl_4$ again serves as the halogen bond donor that produces three different cocrystals based upon isomeric pyridine vinyl esters, namely, (*E*)-methyl-3-(pyridine-X-yl)prop-2-enoate (where X = 4, 3, and 2) (4-PAMe), (3-PAMe), or (2-PAMe) (Scheme 1). The cocrystals $(C_6I_2Cl_4)\cdot$(4-PAMe) and $(C_6I_2Cl_4)\cdot 2$(3-PAMe) both undergo a regioselective photoreaction to yield the corresponding head-to-head photoproducts, namely, (*rctt*)-dimethyl-3,4-bis(pyridine-4-yl)cyclobutane-1,2-dicarboxylate (4,4′-BPCD) and (*rctt*)-dimethyl-3,4-bis(pyridine-3-yl)-cyclobutane-1,2-dicarboxylate (3,3′-BPCD) respectively (Scheme 1). In both cases, the photoreaction did not proceed via a single-crystal-to-single-crystal transformation, since the crystalline state was lost upon exposure to UV light. The third cocrystal $(C_6I_2Cl_4)\cdot$(2-PAMe) was determined to be photostable, since no reaction was observed even after 80 h of irradiation.

The simple incorporation of an oxygen containing functional group has not been extensively studied within halogen bonded cocrystals possibly due to the potential competition between the oxygen atom and other groups such as pyridine nitrogen

Received: December 4, 2019
Revised: February 11, 2020
Published: February 12, 2020

Scheme 1. Components of the Various Cocrystals with the Observed Photoreactivity along with the Regiochemistry of the Photoproducts

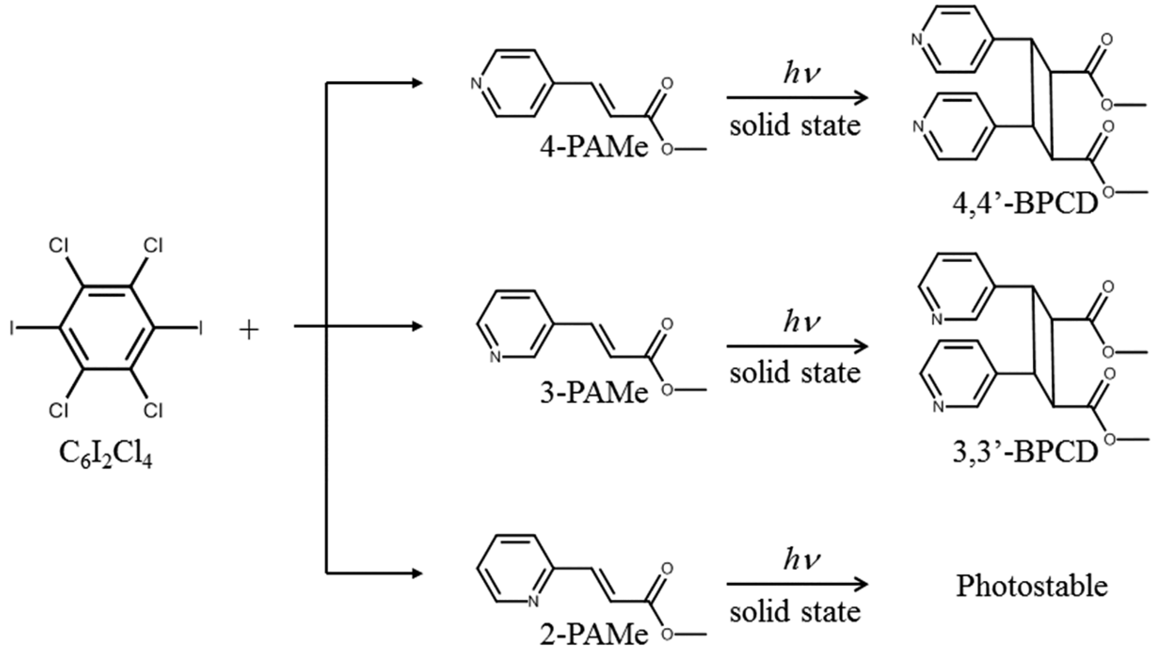

atom as halogen bond acceptors.[10−13] To better evaluate the potential for competitive or cooperative halogen bonding, a series of molecular electrostatic potential calculations utilizing geometry minimization were performed to determine the electrostatic potentials on oxygen atoms and the nitrogen atom on each isomeric ester-containing molecule (Scheme 2). The negative electrostatic potentials on the nitrogen atom and the carbonyl oxygen are comparable. In particular, the pyridine nitrogen was calculated to be slightly more negative when compared to the carbonyl oxygen for 3-PAMe and 4-PAMe but not for 2-PAMe. In addition, the ether oxygen becomes dramatically more negative when the nitrogen atom moves closer to the ester functional group. As a consequence of these electrostatic potentials, it is reasonable to expect that all three heteroatoms could accept halogen and/or hydrogen bonds to form an extended solid.

Scheme 2. Molecular Electrostatic Potential Plots of (a) 4-PAMe, (b) 3-PAMe, and (c) 2-PAMe Shown on the Same Scale Where All Indicated Values Are in kJ/mol

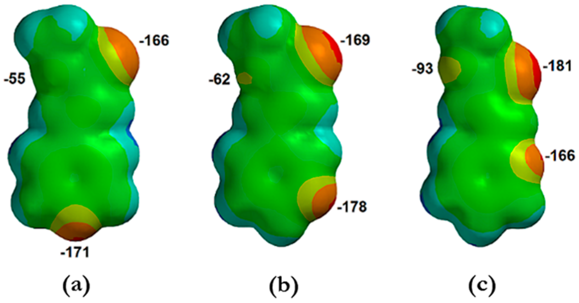

EXPERIMENTAL SECTION

Materials. The solvents toluene and ethanol were both purchased from Sigma-Aldrich Chemical (St. Louis, MO, USA) and used as received. The halogen bond donor 1,4-diiodoperchlorobenzene ($C_6I_2Cl_4$)[14] as well as the ester-based reactant molecules (4-PAMe), (3-PAMe), and (2-PAMe)[15] were synthesized by previously reported methods.

General Methods. All photoreactions were conducted in an ACE Glass photochemistry cabinet using UV-radiation from a 450 W medium-pressure mercury lamp. Each cocrystal was placed between a pair of Pyrex glass plates for irradiation. The photoreactivity and the overall yield for the photoreaction were determined by using ^{1}H NMR spectroscopy on a Bruker Avance 400 MHz spectrometer using DMSO-d_6 as the solvent.

Electrostatic Potential Calculations. The electrostatic potential energy surface for 4-PAMe, 3-PAMe, and 2-PAMe were determined using the Spartan'10 molecular modeling program using density functional theory (DFT) at the B3LYP/6-311++G** level.

Synthesis of ($C_6I_2Cl_4$)·(4-PAMe). The formation of the cocrystal ($C_6I_2Cl_4$)·(4-PAMe) was achieved by dissolving 25 mg of $C_6I_2Cl_4$ in 2 mL of toluene which was then combined with 8.7 mg of 4-PAMe in 2 mL of ethanol (1:1 mol equiv). Crystals suitable for X-ray diffraction formed within 2 days after some evaporation of the solvents.

Synthesis of ($C_6I_2Cl_4$)·2(3-PAMe). In a similar manner as before, the formation of the cocrystal ($C_6I_2Cl_4$)·2(3-PAMe) was realized by dissolving 25 mg of $C_6I_2Cl_4$ in 2 mL of toluene and then combined it with 8.7 mg of 3-PAMe in 2 mL of ethanol (1:1 mol equiv). Again, single crystals suitable for X-ray diffraction formed within 2 days after some loss of solvent via evaporation.

Synthesis of ($C_6I_2Cl_4$)·(2-PAMe). Lastly, the formation of the cocrystal ($C_6I_2Cl_4$)·(2-PAMe) was realized by again dissolving 25 mg of $C_6I_2Cl_4$ in 2 mL of toluene which was then combined with 8.7 mg of 2-PAMe in 2 mL of ethanol (1:1 mol equiv). As before, single crystals suitable for X-ray diffraction formed within 2 days after some evaporation of the two solvents.

Single Crystal X-ray Diffraction Data Collection. A single crystal of each cocrystal and photoproducts were mounted on a MiTeGen cryoloop in a random orientation for X-ray data collection. A Bruker Venture Duo Photon-II single crystal X-ray diffractometer equipped with an Oxford Cryostream device was used for all data collection. Apex II and SAINT software packages were used for data collection and integration, respectively. The data were corrected for systematic errors using SADABS based on the Laue symmetry using equivalent reflections. Structure solution and refinement were carried out using the SHELXTL-PLUS software package. All structures were

Table 1. Crystallographic Diffraction and Refinement Data for All Cocrystals and Photoproducts

cocrystal	$(C_6I_2Cl_4)\cdot(4\text{-PAMe})$	$(C_6I_2Cl_4)\cdot2(3\text{-PAMe})$	$(C_6I_2Cl_4)\cdot(2\text{-PAMe})$	(4,4′-BPCD)	$(C_6I_2Cl_4)\cdot(3,3'\text{-BPCD})$
chemical formula	$C_{30}H_{18}Cl_8I_4N_2O_4$	$C_{24}H_{18}Cl_4I_2N_2O_4$	$C_{15}H_9Cl_4I_2NO_2$	$C_{36}H_{36}N_4O_8$	$C_{24}H_{18}Cl_4I_2NO_4$
crystal system	monoclinic	triclinic	triclinic	monoclinic	monoclinic
space group	*Cc*	$P\bar{1}$	$P\bar{1}$	$P2_1/n$	$P2_1/c$
a/Å	4.0952(2)	4.0647(5)	8.2370(3)	11.2145(16)	14.8816(5)
b/Å	28.2895(10)	9.2406(11)	9.2267(4)	10.2300(14)	10.5023(3)
c/Å	16.7967(6)	37.473(4)	13.1985(5)	15.073(2)	17.5019(6)
α/°	90	87.384(4)	103.098(2)	90	90
β/°	96.9480(10)	88.721(4)	90.168(2)	106.176(6)	99.6340(10)
γ/°	90	80.110(4)	102.568(2)	90	90
V/Å^3	1931.63(14)	1385.0(3)	952.14(7)	1660.8(4)	2696.81(15)
ρ_{calc}/g cm^{-3}	2.169	1.904	2.200	1.305	1.956
T/K	302	290	296	100	100
Z	4	2	2	2	4
radiation type	Mo Kα	Mo Kα	Mo Kα	Mo Kα	Mo Kα
absorption coefficient, μ/mm^{-1}	3.817	2.690	3.872	0.093	2.763
no. of reflections measured	18024	20504	17092	19442	47146
no. of independent reflections	3898	5633	6916	3389	8150
R_{int}	0.0528	0.0670	0.0271	0.1194	0.0330
R_1 ($I > 2\sigma(I)$)	0.0293	0.0826	0.0337	0.0624	0.0265
$wR(F^2)$ ($I > 2\sigma(I)$)	0.0553	0.2204	0.0765	0.1100	0.0479
R_1 (all data)	0.0334	0.0930	0.0550	0.1478	0.0416
$wR(F^2)$ (all data)	0.0577	0.2311	0.0867	0.1346	0.0519
goodness-of-fit	1.109	1.088	1.016	1.028	1.041
CCDC deposition number	1967335	1967336	1967337	1967338	1967339

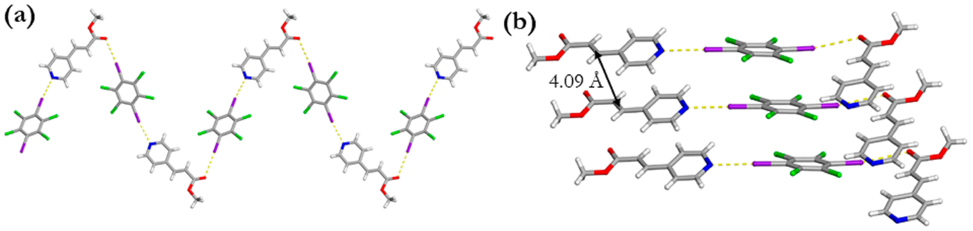

Figure 1. X-ray structure of $(C_6I_2Cl_4)\cdot(4\text{-PAMe})$: (a) wave-like one-dimensional supramolecular polymer based upon I···N and I···O halogen bonds and (b) the homogeneous face-to-face $\pi-\pi$ stacking of the aromatic rings.

solved by direct methods with a full matrix least-squares refinement where all non-hydrogen atoms were refined anisotropically to convergence. In addition, all hydrogen atoms were treated using an appropriate riding model (AFIX m3). X-ray diffraction and refinement data for all cocrystals and photoproducts are given in Table 1.

■ RESULTS AND DISCUSSION

Structure and Photoreactivity of $(C_6I_2Cl_4)\cdot(4\text{-PAMe})$.

Crystallographic analysis determined $(C_6I_2Cl_4)\cdot(4\text{-PAMe})$ crystallized into the centrosymmetric monoclinic space group *Cc*. The asymmetric unit contains a single molecule of both $C_6I_2Cl_4$ and 4-PAMe. The cocrystal is sustained by the combination of I···N [I···N 2.900(6) Å; C−I···N 171.8(2)°] and I···O halogen bonds [I···O 3.224(7) Å; C−I···O 165.0(3)°] that yield a wave-like one-dimensional supramolecular polymer (Figure 1a). The dihedral angle between $C_6I_2Cl_4$ and 4-PAMe via the I···N halogen bond was determined to be 32.2°. The ester group with the electron rich carbonyl oxygen also forms an I···O halogen bond with the second crystallographic unique iodine atom. Molecules of $C_6I_2Cl_4$ are found to engage in a homogeneous $\pi-\pi$ stacking arrangement, similar to that observed in our previous study with the cocrystal $(C_6I_2Cl_4)\cdot(4,4'\text{-BPE})$.[8] This homogeneous stacking is found to be parallel to the crystallographic *a*-axis yielding an infinite column of the halogen bond donor (Figure 1b). Because of crystal symmetry, neighboring pairs of C═C in 4-PAMe molecules are found at a distance of 4.095 Å, which is equal to the distance of the *a*-axis. The position of the C═C within the infinite column meets all of the requirements for a solid-state [2 + 2] cycloaddition reaction as stated by Schmidt.[16]

To determine if a solid-state photoreaction would occur, a powdered sample was then put between glass plates and placed in a photoreactor cabinet to be exposed to broadband UV radiation from a 450 W medium-pressure mercury lamp. The progress of the [2 + 2] cycloaddition reaction was monitored by ^{1}H NMR spectroscopy. A photoreaction was detected as evidenced by the complete loss of the olefinic peaks on 4-PAMe at 6.92 and 7.65 ppm along with the appearance of cyclobutane peaks at 4.11 and 4.33 ppm in the ^{1}H NMR spectrum (Figures S1 and S2). The position of the ^{1}H NMR signal for the cyclobutane ring suggests the photoproduct to be 4,4′-BPCD.[17] The yield for the [2 + 2] cycloaddition reaction was determined, by ^{1}H NMR, to be quantitative after 80 h of irradiation.

To confirm the regiochemistry of the photoproduct, the irradiated powder was dissolved in toluene in order to produce single crystals suitable for X-ray diffraction. In particular, the remaining solid was dissolved in 5 mL of toluene, and within 2 days crystals suitable for X-ray diffraction were realized. In the vial were two distinct crystal morphologies, and, based on the unit cell dimensions, one was determined to be $C_6I_2Cl_4$, while the other was the photoproduct as a single-component solid. The photoproduct crystallized into the centrosymmetric monoclinic space group $P2_1/n$. The asymmetric unit contains a single molecule of 4,4′-BPCD and confirms the head-to-head regiochemistry of the photoproduct (Figure 2a). The three-dimensional structure is sustained by the combination of both C−H···N and C−H···O hydrogen bonds (Figure 2b). The intermolecular C−H···N hydrogen bond [C···N 3.340(4) Å] is observed between an alpha hydrogen on the pyridine ring and the nitrogen atom. Two different types of C−H···O hydrogen bonds were observed within 4,4′-BPCD. First, a C−H···O hydrogen bond [C···O 3.438(4) Å] was observed between an alpha hydrogen on the ring interacting with the carbonyl oxygen. Lastly, a bifurcated C−H···O hydrogen bond [C···O 3.300(4) and 3.461(3) Å] was observed between both a beta hydrogen on the pyridine ring along with a cyclobutane hydrogen bonding with the other unique carbonyl oxygen.

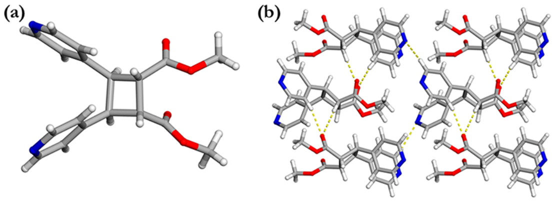

Figure 2. X-ray structure of 4,4′-BPCD: (a) head-to-head regiochemistry of the photoproduct and (b) C−H···N and C−H···O hydrogen bonds yielding a three-dimensional structure.

Structure and Photoreactivity of $(C_6I_2Cl_4)\cdot 2(3\text{-PAMe})$. Crystallographic analysis determined that $(C_6I_2Cl_4)\cdot 2(3\text{-PAMe})$ crystallized into the centrosymmetric triclinic space group $P\bar{1}$. The asymmetric unit contains two different halves of $C_6I_2Cl_4$ and two molecules of 3-PAMe. The cocrystal is sustained by I···N halogen bonds [I···N 2.881(17) and 2.904(17) Å; C−I···N 178.3(5) and 178.5(6)°] where all iodine atoms are interacting with only pyridine nitrogen atoms (Figure 3a). The dihedral angles between $C_6I_2Cl_4$ and the two 3-PAMe molecules via the I···N halogen bond were determined to be 22.3° and 35.3°. A one-dimensional solid is realized due to the C−H···O hydrogen bonds [C···O 3.1530(4) Å] that is found between the gamma hydrogen and the carbonyl oxygen (Figure 3b). As noted in the structure of $(C_6I_2Cl_4)\cdot(4\text{-PAMe})$, molecules of $C_6I_2Cl_4$ are $\pi-\pi$ stacking in a homogeneous pattern forming an infinite column that is parallel to the crystallographic *a*-axis (Figure 3a). Again due to crystal symmetry, neighboring pairs of C═C are parallel and at a distance of 4.065 Å (which is equal to the distance of the *a*-axis) thereby meeting the requirements for a [2 + 2] cycloaddition reaction.[16]

A powdered sample was then placed in a photoreactor, as before, to determine if a solid-state [2 + 2] cycloaddition reaction would occur. Indeed, a photoreaction was confirmed as evidenced by the loss of the olefinic peaks on 3-PAMe at 6.82 and 7.69 ppm along with the concomitant appearance of peaks at 4.14 and 4.35 ppm for the cyclobutane protons in the ^{1}H NMR spectrum (Figures S3 and S4). The location of the ^{1}H NMR signal for the cyclobutane ring suggests that the photoproduct is 3,3′-BPCD.[18] The overall yield for the [2 + 2] cycloaddition reaction was quantitative after 80 h of irradiation as determined by ^{1}H NMR spectroscopy.

To confirm the regiochemistry of the resulting photoproduct, the remaining powder was dissolved in 5 mL of toluene to yield single crystals suitable for X-ray diffraction. The cocrystal $(C_6I_2Cl_4)\cdot(3,3'\text{-BPCD})$ crystallized into the centrosymmetric monoclinic space group $P2_1/c$. The asymmetric unit contains a single molecule of each $C_6I_2Cl_4$ and 3,3′-BPCD and confirms the head-to-head regiochemistry (Figure 4a). The cocrystal is sustained by the combination of I···N halogen bonds and C−H···O hydrogen bonds to yield a two-dimensional structure. The photoproduct 3,3′-BPCD accepts two halogen bonds [I···N 2.901(2) Å; C−I···N 178.50(8)°] to yield a four component assembly due to the head-to-head regiochemistry of the photoproduct. Three different types of C−H···O hydrogen bonds were observed within $(C_6I_2Cl_4)\cdot(3,3'\text{-BPCD})$ (Figure 4b). First, a C−H···O hydrogen bond [C···O 3.307(3) Å] was observed between the hydrogen atom that is para to the nitrogen and the carbonyl oxygen. Next, that same carbonyl oxygen also accepts a C−H···O hydrogen bond [C···O 3.489(3) Å] from the methyl group on the ester group. Lastly, a hydrogen bond [C···O 3.307(3) Å] was observed between a cyclobutane hydrogen and the second unique carbonyl oxygen.

Structure and Photoreactivity of $(C_6I_2Cl_4)\cdot(2\text{-PAMe})$. Single crystal analysis determined the formula of the cocrystal formed with the 2-PAMe isomer to be $(C_6I_2Cl_4)\cdot(2\text{-PAMe})$ that crystallized into the centrosymmetric triclinic space group $P\bar{1}$. The asymmetric unit contains a single molecule of both $C_6I_2Cl_4$ and 2-PAMe. In this cocrystal, the C═C within 2-PAMe are found to be disordered over two positions and after a free variable refinement the occupancies were determined to be .70/.30 at 296 K. Unlike the previous structures, the

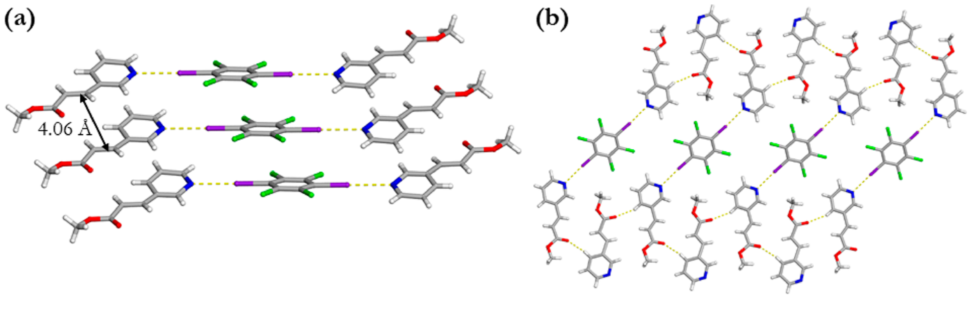

Figure 3. X-ray structure of $(C_6I_2Cl_4)\cdot 2(3\text{-PAMe})$: (a) the homogeneous face-to-face $\pi-\pi$ stacking of the aromatic rings and (b) the two-dimensional sheet held together by both I···N halogen bonds and C−H···O hydrogen bonds.

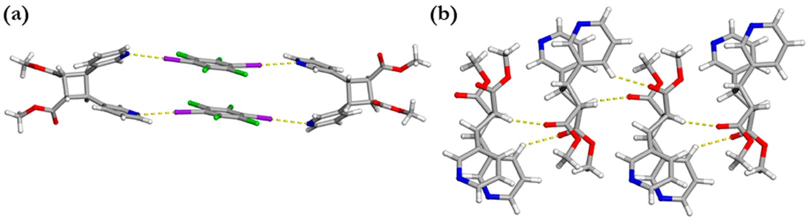

Figure 4. X-ray structure of $(C_6I_2Cl_4)\cdot$(3,3′-BPCD): (a) four-component solid held together by I···N halogen bonds confirming the head-to-head regiochemistry of the photoproduct and (b) C−H···O hydrogen bonds that yields a two-dimensional structure.

existence of both I···N halogen bonds [I···N 2.986(3) Å; C−I···N 174.17(10)°] and I···O halogen bonds [I···O 3.168(3) Å; C−I···O 166.57(9)°] to the ether oxygen was observed which resulted in a one-dimensional structure (Figure 5a). The dihedral angle between the aromatic rings on $C_6I_2Cl_4$ and 2-PAMe via the I···N halogen bond was determined to be 58.6°. In addition, one of the chlorine atoms form a Cl···O halogen bond [Cl···O 3.068(3) Å; C−Cl···O 159.94(13)°] to the carbonyl oxygen to produce a ladder-like structure (Figure 5b). As a consequence of these halogen bonds, a pair of $C_6I_2Cl_4$ molecules are found to be offset but parallel with two unique distances between the iodide atoms to be 4.177 and 4.310 Å. The nearest neighboring 2-PAMe are found to be in a head-to-tail arrangement within the ladder-like structure with a C═C distance between the closest pair to be 3.78 Å (Figure 6).

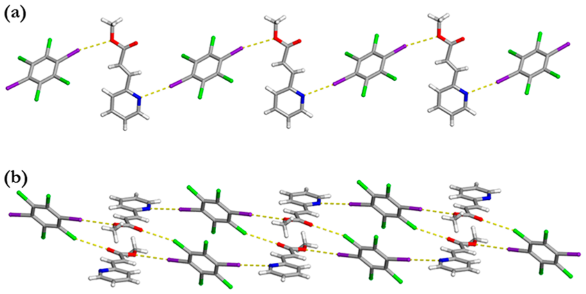

Figure 5. X-ray structure of $(C_6I_2Cl_4)\cdot$(2-PAMe): (a) one-dimensional supramolecular polymer based upon both I···N and I···O halogen bonds and (b) the ladder-like structure illustrating the offset nature of the $C_6I_2Cl_4$ molecules. The observed disorder was removed for clarity.

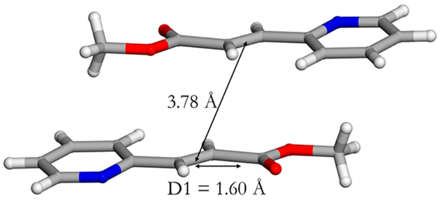

Figure 6. Illustrating the parallel displacement value (D1) for a neighboring pair of C═C in $(C_6I_2Cl_4)\cdot$(2-PAMe). The observed disorder was removed for clarity.

To determine if a solid-state photoreaction would occur within $(C_6I_2Cl_4)\cdot$(2-PAMe), a powdered sample was again exposed to UV radiation within a photoreactor. After 80 h of UV exposure, $(C_6I_2Cl_4)\cdot$(2-PAMe) was found to be photostable since the ^1H NMR spectrum remained unchanged. To understand the structural reason for the observed photostability within $(C_6I_2Cl_4)\cdot$(2-PAMe), a displacement parameter for a pair of C═C was determined. Ramamurthy has previously described geometrical parameters that contribute to a solid's ability or inability to photoreact.[19] Important to this cocrystal is a parameter, D1, that is based upon the displacement of a pair of C═C parallel to the molecular axis. Calculating the D1 value within $(C_6I_2Cl_4)\cdot$(2-PAMe) resulted in a value of 1.60 Å, which does not allow for complete overlap of the orbitals in the nearest neighboring pair of C═C (Figure 6). This large value is believed to be the cause for the observed photostability for this cocrystal.

■ CONCLUSION

In this paper, we report the ability to form a pair of photoreactive cocrystals based upon a series of isomeric pyridine vinyl esters that utilize halogen bonding interactions. In both cases, a quantitative regioselective photoreaction was observed yielding only the head-to-head photoproduct. Currently, we are trying to identify additional organic functional groups that can be included within photoreactive halogen bonded cocrystals. In addition, we are also investigating the use of similar shaped halogen bond donors, such as 1,4-diiodoperfluorobenzene, to determine if it would also template solid-state photoreactions.

■ ASSOCIATED CONTENT

Supporting Information

The Supporting Information is available free of charge at https://pubs.acs.org/doi/10.1021/acs.cgd.9b01624.

Experimental details, X-ray crystallographic data, and ^1H NMR spectra for all photoreactive cocrystals (PDF)

Accession Codes

CCDC 1967335−1967339 contain the supplementary crystallographic data for this paper. These data can be obtained free of charge via www.ccdc.cam.ac.uk/data_request/cif, or by emailing data_request@ccdc.cam.ac.uk, or by contacting The Cambridge Crystallographic Data Centre, 12 Union Road, Cambridge CB2 1EZ, UK; fax: +44 1223 336033.

■ AUTHOR INFORMATION

Corresponding Authors

Eric Bosch − *Department of Chemistry, Missouri State University, Springfield, Missouri 65897, United States;* orcid.org/0000-0002-6465-1879; Phone: +1 417-836-4277; Email: ericbosch@missouristate.edu
Ryan H. Groeneman − *Department of Biological Sciences, Webster University, St. Louis, Missouri 63119, United States;* orcid.org/0000-0002-4602-6287; Phone: +1 314-246-7466; Email: ryangroeneman19@webster.edu

Authors

Samantha J. Kruse − *Department of Biological Sciences, Webster University, St. Louis, Missouri 63119, United States;* orcid.org/0000-0003-4261-2024

Fayeshun Brown − *Department of Biological Sciences, Webster University, St. Louis, Missouri 63119, United States*

Complete contact information is available at:
https://pubs.acs.org/10.1021/acs.cgd.9b01624

Notes

The authors declare no competing financial interest.

■ ACKNOWLEDGMENTS

R.H.G. gratefully acknowledges financial support from Webster University in the form of various Faculty Research Grants. Funding from the National Science Foundation (MRI, CHE-1827756) for the purchase of the Bruker Venture Duo Photon-II diffractometer is also acknowledged.

■ REFERENCES

(1) Cavallo, G.; Metrangolo, P.; Milani, R.; Pilati, T.; Priimagi, A.; Resnati, G.; Terraneo, G. The Halogen Bond. *Chem. Rev.* **2016**, *116*, 2478.

(2) Gilday, L. C.; Robinson, S. W.; Barendt, T. A.; Langton, M. J.; Mullaney, B. R.; Beer, P. D. Halogen Bonding in Supramolecular Chemistry. *Chem. Rev.* **2015**, *115*, 7118.

(3) Corpinot, M. K.; Bučar, D.-K. A Practical Guide to the Design of Molecular Crystals. *Cryst. Growth Des.* **2019**, *19*, 1426.

(4) Priimagi, A.; Cavallo, G.; Metrangolo, P.; Resnati, G. The Halogen Bond in the Design of Functional Supramolecular Materials: Recent Advances. *Acc. Chem. Res.* **2013**, *46*, 2686.

(5) Sinnwell, M. A.; Blad, J. N.; Thomas, L. R.; MacGillivray, L. R. Structural flexibility of halogen bonds showed in a single-crystal-to-single-crystal [2 + 2] photodimerization. *IUCrJ* **2018**, *5*, 491.

(6) Sinnwell, M. A.; MacGillivray, L. R. Halogen-Bond Templated [2 + 2] Photodimerization in the Solid State: Directed Synthesis and Rare Self-Inclusion of a Halogenated Product. *Angew. Chem., Int. Ed.* **2016**, *55*, 3477.

(7) Caronna, T.; Liantonio, R.; Logothetis, T. A.; Metrangolo, P.; Pilati, T.; Resnati, G. Halogen Bonding and $\pi\cdots\pi$ Stacking Control Reactivity in the Solid State. *J. Am. Chem. Soc.* **2004**, *126*, 4500.

(8) Bosch, E.; Kruse, S. J.; Krueger, H. R., Jr.; Groeneman, R. H. Role of π-π Stacking and Halogen Bonding by 1,4-Diiodoperchlorobenzene to Organize the Solid State to Achieve a [2 + 2] Cycloaddition Reaction. *Cryst. Growth Des.* **2019**, *19*, 3092.

(9) Bosch, E.; Kruse, S. J.; Reinheimer, E. W.; Rath, N. P.; Groeneman, R. H. Regioselective [2 + 2] cycloaddition reaction within a pair of polymorphic co-crystals based upon halogen bonding interactions. *CrystEngComm* **2019**, *21*, 6671.

(10) Nemec, V.; Fotović, L.; Vitasović, T.; Cinčić, D. Halogen bonding of the aldehyde oxygen atom in cocrystals of aromatic aldehydes and 1,4-diiodotetrafluorobenzene. *CrystEngComm* **2019**, *21*, 3251.

(11) Nemec, V.; Fotović, L.; Friščić, T.; Cinčić, D. A Large Family of Halogen-Bonded Cocrystals Involving Metal−Organic Building Blocks with Open Coordination Sites. *Cryst. Growth Des.* **2017**, *17*, 6169.

(12) Goodwin, M. J.; Steed, B. W.; Yufit, D. S.; Musa, O. M.; Berry, D. J.; Steed, J. W. Halogen and Hydrogen Bonding in Povidone-Iodine and Related Co-Phases. *Cryst. Growth Des.* **2017**, *17*, 5552.

(13) Zbačnik, M.; Vitković, M.; Vulić, V.; Nogalo, I.; Cinčić, D. Competition between Halogen Bonds in Cocrystals of Imines Derived from *o*-Vanillin. *Cryst. Growth Des.* **2016**, *16*, 6381.

(14) Reddy, C. M.; Kirchner, M. T.; Gundakaram, R. C.; Padmanabhan, K. A.; Desiraju, G. R. Isostructurality, polymorphism and mechanical properties of some hexahalogenated benzenes: the nature of halogen···halogen interactions. *Chem. - Eur. J.* **2006**, *12*, 2222.

(15) Agarwal, K. C.; Knaus, E. E. Synthesis and reactions of heterocyclic methyl 2-propenoates and 2,3-epoxypropanoates with nucleophiles. *J. Heterocycl. Chem.* **1985**, *22*, 65.

(16) Schmidt, G. M. J. Photodimerization in the Solid State. *Pure Appl. Chem.* **1971**, *27*, 647.

(17) Elacqua, E.; Kaushik, P.; Groeneman, R. H.; Sumrak, J. C.; Bučar, D.-K.; MacGillivray, L. R. A Supramolecular Protecting Group Strategy Introduced to the Organic Solid State: Enhanced Reactivity through Molecular Pedal Motion. *Angew. Chem., Int. Ed.* **2012**, *51*, 1037.

(18) Elacqua, E.; Groeneman, R. H.; Reinheimer, E. W.; Bučar, D.-K.; MacGillivray, L. R. Organosulfonates Aid Argentophilic Forces in the Crystal Engineering of [2 + 2] Photodimerizations: Reactivity Involving 3-Pyridyl Groups. *Supramol. Chem.* **2014**, *26*, 207.

(19) Ramamurthy, V.; Venkatesan, K. Photochemical reactions of organic crystals. *Chem. Rev.* **1987**, *87*, 433.